ORIGINAL ARTICLE

Journal of Cachexia, Sarcopenia and Muscle 2015; **6**: 365–380
Published online 23 May 2015 in Wiley Online Library (wileyonlinelibrary.com) **DOI:** 10.1002/jcsm.12031

Activin-β_C modulates cachexia by repressing the ubiquitin-proteasome and autophagic degradation pathways

Francesco Elia Marino[1*], Gail Risbridger[2] & Elspeth Gold[1*]

[1]*Department of Anatomy, University of Otago, Dunedin, New Zealand;* [2]*Department of Anatomy and Developmental Biology, Monash University, Clayton, Victoria, Australia*

Abstract

Background Cancer-associated cachexia and muscle wasting are considered key determinants of cancer-related death and reduction in the quality of life of cancer patients. A crucial link has been established between activin signaling and skeletal muscle atrophy-hypertrophy.
We previously showed that activin-β_C, a novel activin-A antagonist, is a tumor modulator that abolishes the cancer-associated cachexia in a mouse genetic model of gonadal tumorigenesis, in which the normal balance of inhibin/activin signalling is disrupted by a targeted mutation in the *Inha* gene (inhibin α-KO mouse). This study aimed to identify the molecular mechanism by which activin-β_C increases survival and abolishes cancer-associated cachexia in α-KO mice. We hypothesized that overexpression of activin-β_C modulates the cachexia phenotype by antagonizing the activin signaling pathway and repressing muscle wasting via the ubiquitin-proteasome and the autophagic-lysosomal degradation pathways.

Methods Male and female ActC++, α-KO, and α-KO/ActC++ mice and WT littermate controls were studied. Western blot analysis for the specific E3 ubiquitin ligases, atrogin-1 and MuRF1, markers of the autophagic-lysosomal pathway, Beclin-1, p62, and LC3A/B, effectors Smad-2, Smad-3 and myostatin was performed in the gastrocnemius of age-matched mice. Histopathology of the gastrocnemius and survival analysis were also conducted in animals from the same breeding cohort. Serum levels of activin-A, inflammatory cytokines, hormonal profile, and bone density were also assessed.

Results Increased levels of atrogin-1, MuRF-1, Beclin-1, p62, LC3A/B-I, Smad-2 and serum levels of activin-A were noted in the α-KO mice. These mice developed gonadal cancers followed by severe weight loss, and reduced survival. Overexpression of activin- β_C antagonized the activin signaling cascade, attenuating the ubiquitin-proteasome and the autophagic-lysosomal degradation pathways, and reduced serum levels of activin-A. α-KO/ActC++ mice displayed a less aggressive cachectic phenotype, reduced tumor weight, and prolonged survival.

Conclusion Our findings show for the first time a specific effect of activin-β_C on muscle wasting and transcription factors involved in muscle protein degradation. The study indicates that activin-β_C may be a novel therapy to abrogate cancer-associated weight loss and prolong survival.

Received: 3 November 2014; Revised: 21 January 2015; Accepted: 13 February 2015
**Correspondence to: Elspeth Gold and Francesco Elia Marino, Department of Anatomy, University of Otago, PO Box 913, Dunedin, 9054, New Zealand: Tel: +64 3 479 5647, Fax: + 63 3 479 7254, Email: Elspeth.Gold@otago.ac.nz; francescoelia.marino@otagoanatomy.com*

Introduction

Cancer cachexia has been recently defined as a syndrome affecting the majority of cancer patients with advanced cancer and is associated with a reduction in treatment tolerance, response to therapy, quality of life, and survival. The clinical manifestation of cachexia is characterized by skeletal muscle wasting with or without loss of fat mass, and it is often associated with psychological distress, fatigue, and deterioration in physical function.[1]

Management of cancer cachexia is clinically challenging because of the absence of established therapeutic protocols to treat this multifaceted syndrome. Only two therapies, resulting from randomized trials, are available to treat cancer-associated cachexia: corticosteroids and progestins.[2] However, neither of these drugs has a significant effect on muscle loss, and the side effects associated with their administration limit long-term use. Development of new drugs to target cancer cachexia is extremely difficult because of the complicated pathogenesis of this condition.

Several hormones, cytokines, and tumor-derived factors have been shown to influence the pathogenesis of muscle wasting and cancer-associated cachexia. For example, inflammation and inflammatory response to the tumor are factors participating in the development of cancer-associated cachexia.[3] In the last two decades, different catabolic mediators (both humoral and tumoral) involved in cancer have been considered as targets for clinical investigations and/or therapeutic strategies without a significant improvement in the clinical management of cancer-associated weight loss.

The TGF-β family of ligands, including myostatin, activin-A, and Growth Differentiation Factor 11 (GDF11) and the receptors mediating signaling in particular the ActRIIB (a high-affinity activin type-II receptor in muscle), have been shown to have a crucial role in regulating muscle growth.[4]

Transgenic mice expressing a negative dominant ActRIIB display skeletal muscle hypertrophy.[5,6] Additionally, in the inhibin-α deficient mouse model (α-KO), where activins are deregulated because of the loss of the inhibin-αsubunit, gonadal tumours and a cachexia phenotype can be observed.[7] Lee and co-workers provided the first demonstration that the soluble receptor ActRIIB induces muscle hypertrophy in vivo[8]. Additionally, Klimek and colleagues showed that preservation of muscle wasting could be obtained using a soluble form of the ActRIIB[9]. Zhou *et al.* have showed the potential therapeutic benefit of blocking the activin signalling through ActRIIB in cancer cachexia. Administration of a decoy receptor to antagonize the ActRIIB pathway in four distinct models of lethal cachexia prevented further skeletal muscle wasting and reversed weight loss, leading to a significant increase in survival compared with the tumor-bearing control animals that did not receive the decoy receptor.[10]

Activin-A and myostatin are sufficient to induce skeletal muscle atrophy, initiating a signalling cascade leading to activation of Forkhead box (FOXO) and nuclear factor kappa-light–chain-enhancer of activated B cells (NF-kB) involving Smad transcription factors.[11,12] FOXO3 by itself has been shown to regulate a set of atrophy-associated genes, in particular the muscle-specific ubiquitin ligases (E3s), muscle RING-finger 1 (MuRF1), and atrogin-1/MAFbx, which are associated with increased degradation of myofibrillar proteins through the ubiquitin-proteasome pathway.[11]

The importance of these proteins has been clearly shown in mice lacking either enzymes, where the loss of muscle mass upon denervation is significantly reduced.[13]

Additionally, recent studies have also suggested that the autophagic-lysosomal pathway is a key contributor to skeletal muscle depletion and that the balance between synthesis and degradation determines the final net muscle protein turnover.[14–17] Penna *et al.* recently showed that the autophagic-lysosomal pathway is activated in the skeletal muscle of the C26-bearing mice but not in sarcopenic animals, suggesting that different mechanism might be operating in muscle wasting secondary to cancer cachexia vs. sarcopenia.[17]

Our group described for the first time a novel regulator of activin-A bioactivity: activin-β_C.[18] We previously showed that up-regulation of activin-β_C reduces progression of Sertoli and granulosa cell tumours, abrogating the cachexia-like syndrome in the inhibin deficient mice (α-KO) and increasing survival rates.[19] These findings suggested that the activin-β_C subunit plays an important role in activin-A antagonism.

Therefore, this study was designed to determine the molecular mechanism by which activin-β_C abrogated cancer cachexia and increased survival in the α-KO mice. Specifically, we aimed to determine whether overexpression of activin-β_C was sufficient to regulate protein expression of factors involved in protein degradation, focusing our attention on the ubiquitin-proteasome catabolic system and the autophagic-lysosomal pathways. We also explored the impact of activin-β_C on the inflammatory (IL-6, IFN-γ, and TNF-α) and hormonal profile of these mice, and we assessed its impact on bone density.

Material and methods

Experimental animals

All experiments were approved by the Animal Ethics Committee of the University of Otago and conducted in accordance with the New Zealand code of practice in adherence with the National Institutes of Health (NIH) guide for the care and use of laboratory animals. All animals were housed under a 12:12 h light–dark cycle, food and water were available *ad libitum*. Mice on C57BL/6 background were originally purchased from Jackson Laboratories (Bar Harbor, ME) and bred at the University of Otago. α-KO mice were kindly provided by Professor Martin Matzuk (Baylor College of Medicine Houston).

Human activin-β_C (under the control of a CMV promoter) - overexpressing mice (ActC++) were obtained from Monash University, Australia.[18] To obtain the α-KO/ActC++ mice, heterozygous α-KO mice were crossed with double heterozygous ActC++ mice.[19] A competitive genomic PCR screening strategy with specific primers was used to confirm positive progeny.[18,20]

Animals were allocated in the experimental groups as follows: Male mice WT $n = 8$, ActC++ $n = 8$, α-KO $n = 5$, α-KO/ActC++ $n = 4$; Female mice WT $n = 8$, ActC++ $n = 8$, α-KO $n = 5$, α-KO/ActC++ $n = 5$. For the stereological, serum, western blot, and bone density analyses, 8 week-old animals (WT, ActC++, α-KO, and α-KO /ActC++) were used, as 100% survival rate was noted at this time point for all experimental groups. Four animals, randomly selected from each experimental group, were used for the stereological and western blot analyses. Serum analysis was conducted in three animals, randomly selected from each experimental group.

Mouse monitoring

Changes in body weight, tumor mass, BAR (bright, alert, and responsive) score, general clinical signs (inactive, hunched posture, coat rough-fun on end, red eye/nose discharges, pink staining of the neck, and dehydration), behavioural signs of pain, and water balance were monitored daily. Animals were sacrificed when one of the following humane end-points was observed: (i) weight loss of 10% or more over 24 h; (ii) weight loss of 20% or more plus one other clinical sign compared with the control group; and (iii) weight loss of 25% compared with the control group.

Tissue collection

Animals were anaesthetized and serum obtained by cardiac puncture. Animals were then euthanized by cervical dislocation. Tail biopsy was obtained and snap frozen to confirm genotype of interest. The α-KO and α-KO/ActC++ mice were sacrificed at 12–17 weeks of age, based on their survival rates and when clinical manifestation of any of the human end-points reported earlier was recorded. WT and ActC++ mice survived up to 30 weeks of age.

When animals were sacrificed, testis, ovary, gastrocnemius, and femur were collected. Part of the gastrocnemius was snap frozen for further analysis, the remaining part of the gastrocnemius was stored in Bouin's solution for 4–6 h and then transferred to 70% ethanol for 12–24 h, embedded in paraffin, sectioned and mounted on Superfrost microscope slides (Menzel-Glaser).

Stereological analysis

Serial sections were stained with hematoxylin and eosin and photographed on an Olympus microscope (40x objective). Average fiber area in gastrocnemius muscles was calculated by counting 200–300 fibers in transverse section of muscles from four mice for each genotype and calculating the average total area of the counted fibers normalized by the number of counted fibers.[21]

Western blot analysis

Frozen tissues from four animals per group were homogenized with the Tissue Lyser II (Qiagen Cat # 85300) for 5 min at 30 Hz in ice-cold RIPA Buffer [150 mM NaCl, 1.0% IGEPAL® CA-630, 0.5% sodium deoxycholate, 0.1% SDS, 50 mM Tris pH 8.0 (Sigma-Aldrich Cat R0278)] containing protease and phosphates inhibitor (Thermo Scientific cat 78440) according to the manufacturer's instructions, and the whole homogenate was used for further analysis. Sample protein concentration was determined using the BCA Protein Assay Reagent KIT (Thermo Scientific cat 23225), and equivalent amounts of protein from each sample (40 μg) were subjected to electrophoretic separation on 12% SDS-PAGE acrylamide gels in Tris-Glycine-SDS Running. Following electrophoresis separation, proteins were transferred to a nitrocellulose membrane (GE Healthcare cat 10600003) in Transfer Buffer (250 mM Tris, 1.92 M Glycine, 10% Methanol), blocked with Odyssey Blocking buffer (Li-Cor cat 927–40000) for 1 h, followed by an overnight incubation with primary antibody dissolved in Odyssey blocking buffer containing 0.2% Tween-20 (Sigma-Aldrich cat P2287). Antibodies used were the following: Atrogin-1 (ECM Bioscience cat AP 2041), Murf-1 (ECM Bioscience cat MP3401), Beclin-1 (Abcam cat 55878), SQSTM1/p62 (Abcam cat 91526), LC3A/B (Abcam cat 62721), Myostatin (Abcam cat 71808), Smad 2 (Abcam cat 47083), p-Smad-2 (Abcam cat 53100), Smad-3 (Abcam cat 40854), p-Smad3 (Abcam cat 51451), and GAPDH (Abcam cat 9484).

After an overnight incubation, blots were incubated with secondary antibodies diluted in Odyssey Blocking Buffer for 1 h at room temperature. Secondary antibodies used were the following: IRDye 800CW Goat Anti-Rabbit IgG, H+L (Li-cor cat 926–32211) and IRDye 680LT Goat Anti-Mouse IgG_{2b} (Li-cor cat 926–68052).

Densitometry measurements were performed using the software Image Studio Lite v4.0 (Li-cor) by determining the signal intensity of each band after a background optimization and normalizing to Glyceraldehyde 3-phosphate dehydrogenase (GAPDH). Averaged values from three independent experiments were used for the final statistic analysis.

Inflammatory cytokines were assessed using 0.5 μl of serum, electrophoresed on a 12% SDS-PAGE acrylamide gels and probed with primary and secondary antibodies following exactly the same protocol reported in the preceding paragraph.[22] Antibodies used were as follows: IL-6 (Abcam cat 6672), IFN-γ (Abcam cat 133566) and TNF- α (Abcam cat 9739). Signal intensity of each band was normalized to the mouse IgG2b fraction.

Bone analysis

Skin was removed from the euthanized animal, using a scalpel to cut the cartilage between the femur and tibia; the muscle from femur and around hip joint was removed. The bone isolated was cleaned and stored at −80° in PBS soaked gauze. Femur X-Ray images were acquired using the *In Vivo* MS FX PRO (Bruker). X-Rays were generated at 35 KV (Filter 0.4 mm, fstop 2.80, FOV 200). Bone density was calculated according to manufacturer's guidelines.

Testosterone, estradiol and activin-a ELISA

Serum levels of Testosterone and Estradiol were assessed from three males and three female per group using Abcam Elisa kits (cat 108666 and 108667), according to the manufacturer's instructions. Serum levels of Activin A were assessed from three animals per group using the Quantikine ELISA from (R&D cat DAC00B), according to the manufacturer's instructions.

Statistical analysis

Statistical analysis was conducted using One-Way ANOVA, followed by Tukey's correction for confidence intervals and significance (GraphPad Prism, version 5). For the survival analysis, the Log-rank (Mantel–Cox) test was used. Statistical significance was assumed if P was <0.05.

Results

Activin-β_C overexpression modulates gonadal tumours, reduces activin-A levels, and prolongs survival in the α-KO mice

The α-KO mice developed Sertoli and granulosa cell tumours, leading to a lethal wasting syndrome characterized by progressive weight loss and death. At 8 weeks of age, there was an increase in testis (322 ± 30 mg, $P < 0.0001$) and ovarian weights (34 ± 1 mg, $P < 0.0001$) in the α-KO mice compared with WT controls (testis 107 ± 30 mg, ovary 8 ± 1).

By 8 weeks, the tumor-associated increase weight was reduced in the α-KO /ActC++ mice vs. the α-KO counterpart, with testicular (180 ± 40 mg) weight not statistically different from WT controls. (*Figure* 1A and 1B).

The serum levels of activin-A in the α-KO mice were significantly elevated in both males (4213 ± 50.53 vs. 134.5 ± 31.45 pg/ml) and females (4257 ± 126.8 vs. 204.5 ± 37.42 pg/ml) compared with the WT age-matched controls. However, in the α-KO/ActC++ mice, the serum levels of activin-A were reduced in both male (1392 ± 116.4 pg/ml) and female mice (3182 ± 199.5 pg/ml) compared with the α-KO mice (*Figure* 1C and 1D).

As shown in *Figure* 1E and 1F, overexpression of activin-β_C in the α-KO mice increased survival in both male and female mice. At 13 weeks, 49% of male α-KO/ActC++ mice survived vs. 0% of the α-KO group (chi square 33.95, $P < 0.0001$) *Figure* 1E. At 15 weeks, 56% of female α-KO /ActC++ mice survived vs. 0% of the α-KO mice (chi square 31.22, $P < 0.0001$) *Figure* 1F.

At 12–17 weeks of age, despite a significant difference in the ovarian weights between the α-KO and α-KO/ActC++ mice, there was no significance in testicular weights between these two groups (*Figure* S1A and 1B), thus suggesting that activin-β_C delayed but not completely abolished tumor growth.

Activin-β_C overexpression reduces elevated levels of inflammatory cytokines IL-6, IFN-γ, and TNF-α in the α-KO mice

Elevated levels of IL-6, IFN-γ, and TNF-α were found in both male and female α-KO mice compared with the age-matched WT group. Male mice: IL-6 (3.30 ± 0.32 $P < 0.01$), IFN-γ (3.48 ± 0.48 $P < 0.01$), and TNF-α (3.52 ± 0.17 $P < 0.01$). Female mice IL-6 (3.81 ± 0.69 $P < 0.01$), IFN-γ (4.35 ± 0.56 $P < 0.001$), and TNF-α (8.0 ± 0.79 $P < 0.001$). Overexpression of activin-β_C reduced the high levels of cytokines noted in the α-KO mice; in fact, no statistical significance was found in the cytokines levels of both male and female α-KO/ActC++ mice compared with the WT age-matched control, except for the IFN-γ in the female mice (82.62 ± 0.29 $P < 0.01$). When the cytokine levels in the α-KO/ActC++ mice were compared with the α-KO mice, statistically reduced levels were noted in all groups (*Figure* 2A and 2B).

Activin-β_C overexpression attenuates the ubiquitin proteasome and the autophagy–lysosomal pathway activation and abrogates the reduction in muscle cross-sectional area noted in the α-KO mice.

In different conditions of muscle atrophy, there is an acceleration of the muscle proteolysis mediated by the proteasome ubiquitin pathway and it is demonstrable on muscle extracts.[10,23,24] The catabolic factors Atrogin-1 and MuRF1 involved in the ubiquitin-proteasome pathway were assessed in the gastrocnemius of the α-KO mice in order to determine if any change was present in the α-KO/ActC++ mice. Additionally, three of the most representative markers of the autophagic-lysosomal degradation pathway were assessed: Beclin-1 as an indicator of autophagy induction, LC3A/B to measure autophagosome abundance, and p62/SQSTM1 as a marker of substrate sequestration and eventual degradation.[17]

Figure 1 Activin-β_C overexpression modulates gonadal tumours, reduces activin-A levels, and prolongs survival in the α-KO mice. Changes in testicular (A) and ovarian (B) weights in male and female α-KO and α-KO/Actc++ mice. Age-matched WT and ActC++ controls are also shown. 8 week-old mice *n* = 4–8 per group. Changes in serum activin-A levels in male (C) and female (D) α-KO/ActC++ vs. α-KO mice. Age-matched WT and ActC++ controls are also shown. 8 week-old mice *n* = 3 per group. Survival analysis in male (E) and female (F) α-KO /ActC++ vs. α-KO mice. WT and ActC++mice (30 week-old) are also shown. α-KO and α-KO/ActC++ mice were monitored up to 18 weeks when survived. *n* = 4-8 per group. Values are mean ± SEM. ns = $P > 0.05$; * $P \leq 0.05$; $P \leq 0.01$; *** $P \leq 0.001$; **** $P \leq 0.0001$**

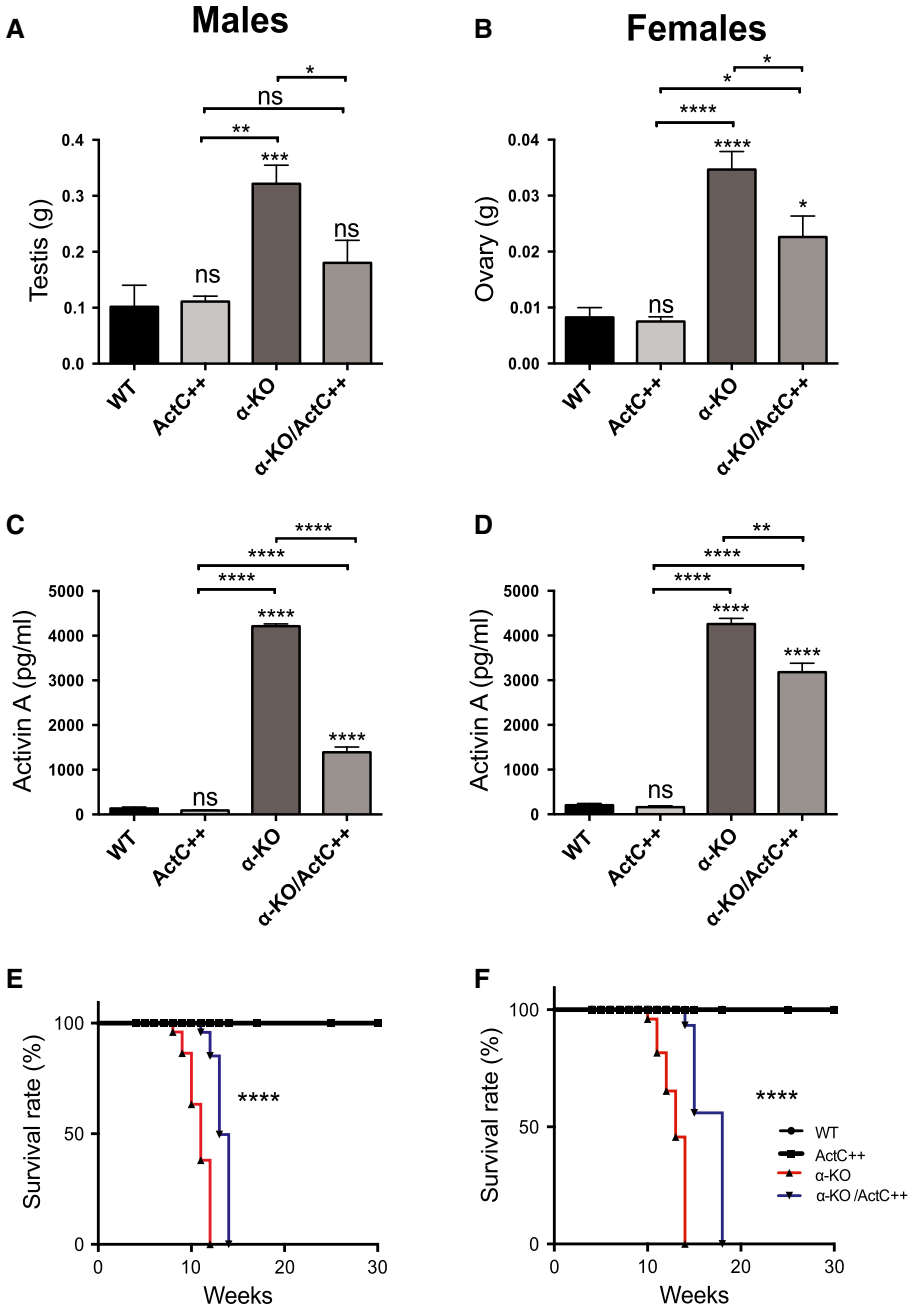

As shown in *Figure* 3, there was a clear increase in Atrogin-1 and MuRF1 in both male (*Figure* 3A) (Atrogin-1 1.60 ± 0.60 $P < 0.05$; MuRF-1 1.90 ± 0.60 $P < 0.01$) and female (Atrogin-1 2.00 ± 0.30 $P < 0.01$; MuRF-1 1.80 ± 0.17 $P < 0.01$) α-KO mice vs. WT age-matched controls (*Figure* 3B).

Beclin-1, an upstream regulator of autophagic sequestration,[25] was increased in both male (2.15 ± 0.31 $P < 0.0001$) and female α-KO (1.48 ± 0.28 $P < 0.05$) vs. the WT age-matched controls, suggesting an activation of the autophagy pathway (*Figure* 4A and 4B).

DOI: 10.1002/jcsm.12031

Figure 2 Activin-β_C overexpression reduces elevated levels of inflammatory cytokines IL-6, INF-γ, and TNF-α in the α-KO mice. Quantification of western blots signal intensities for inflammatory cytokines IL-6, INF-γ and TNF-α in the WT, ActC++, α-KO and α-KO /ActC++ mice are shown. 8 week-old males (a) and females (b) mice *n* = 4 per group. Normalized values are expressed as relative intensities (800 nm channel/700nm channel) to WT. Signals from IL-6, INF-γ and TNF-α appear as green fluorophores and signals from Mouse IgG2b appear as red fluorophores. Values are mean ± SEM. ns = $P > 0.05$; * $P \leq 0.05$; ** $P \leq 0.01$; *** $P \leq 0.001$; **** $P \leq 0.0001$.

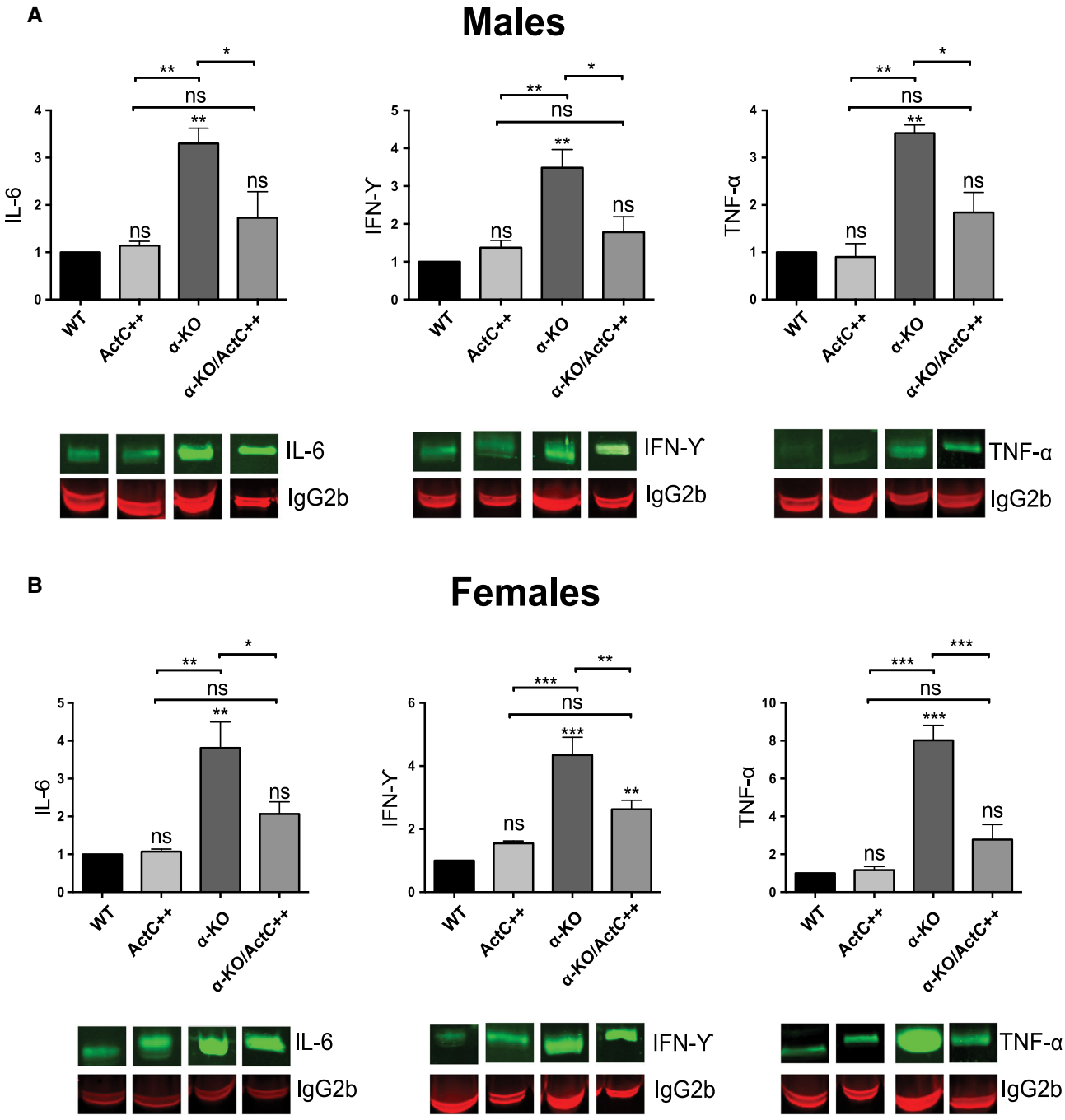

p62, measured as measure of substrate sequestration into autophagosomes (p62 binds LC3 and substrates marked for degradation by ubiquitinilation[26]), was elevated in both male (1.28 ± 0.14 $P < 0.01$) and female α-KO (1.18 ± 0.11 $P < 0.05$) vs. WT age-matched controls (*Figure* 4A and 4B).

The levels of microtubule-associated protein 1 light chain 3A/B isoform I (LC3A/B-I) was elevated in both male (2.69 ± 0.86 $P < 0.01$) and female α-KO (3.31 ± 0.74 $P < 0.0001$) vs. WT age-matched controls, whereas no statistical differences were noted for the levels of LC3A/B-II in both male and female mice (*Figure* 5A and 5B).

Figure 3 Activin-β_C overexpression attenuates Atrogin-1 and MuRF-1 levels in the α-KO mice. Quantification of western blots signal intensities for catabolic factors Atrogin-1 and MuRF-1 in the gastrocnemius of 8 week-old males (a) and females (b) mice $n = 4$ per group. Normalized values are expressed as relative intensities (800 nm channel/700 nm channel) to WT. Signals from Atrogin-1 and MuRF-1 appear as green fluorophores, and signals from GAPDH appear as red fluorophores. Values are mean ± SEM. ns = $P > 0.05$; * $P \leq 0.05$; ** $P \leq 0.01$; *** $P \leq 0.001$; **** $P \leq 0.0001$.

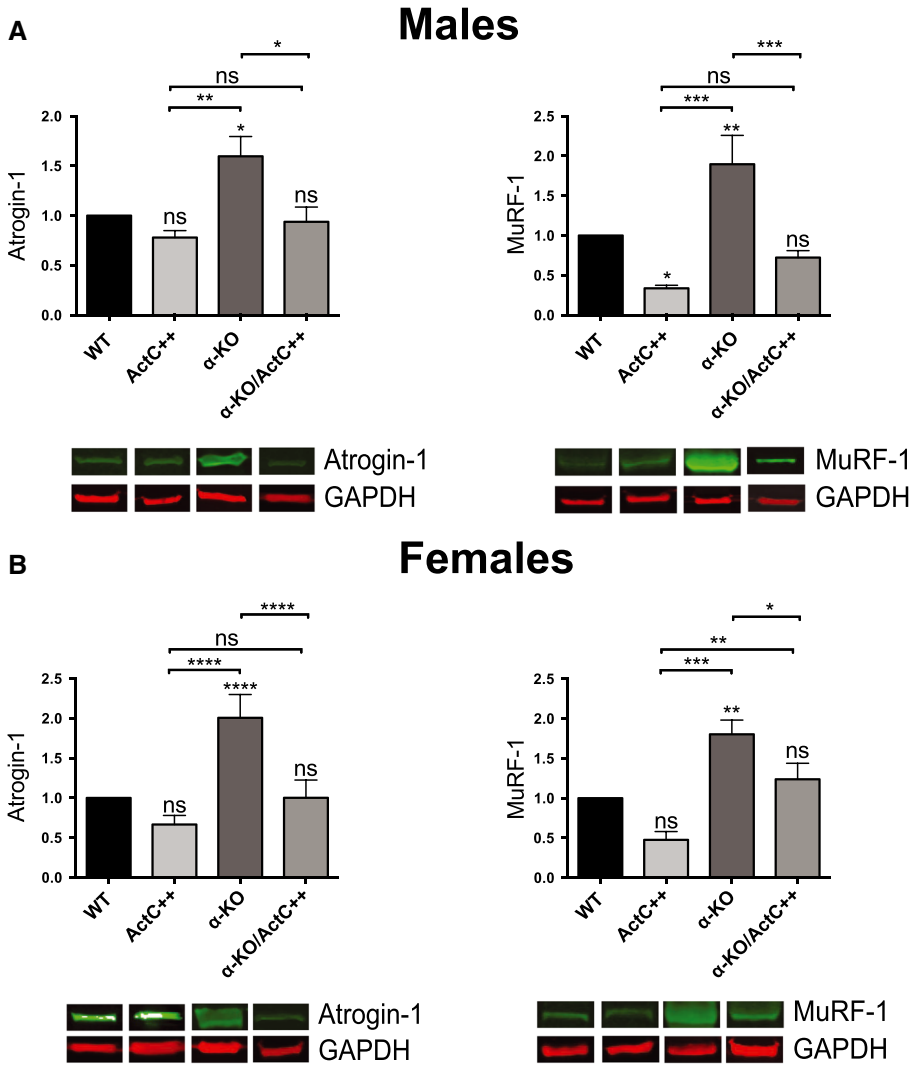

Overexpression of activin-β_C prevented the rise in Atrogin-1 and MuRF1 in both sexes. In fact, in the α-KO/ActC++ mice, except for MuRF1 in the female group, the levels of Atrogin-1 and MuRF1 were not statistically significant compared with WT age-matched controls.

Additionally, overexpression of activin-β_C prevented the rise in Beclin-1 and p62 in both sexes and the rise of LC3A/B-I in the male group. The levels of Beclin-1 and p62 in the α-KO/ActC++ mice were not statistically significant compared with WT age-matched controls. The levels of LC3A/B-I were not statistically significant in the male α-KO/ActC++ group only compared with WT age-matched controls.

To explore the mechanism by which activin-β_C overexpression regulates the atrophy-specific ubiquitin ligases, we assessed the levels of myostatin in order to investigate its potential contribution to the activation of the ubiquitin proteasome pathway activation, and we also assessed Smad levels across the groups analyzed. We investigated both Smad-2 and Smad-3 intracellular effectors. No statistical differences in the levels of myostatin were found in both male and female mice (*Figure* 6A and 6B).

Phospho Smad-2/Smad-2 was markedly increased in the α-KO mice, and overexpression of activin-β_C blocked this increase in both male (*Figure* 7A) and female mice (*Figure* 7B). No statistically significant changes were noted in the phosphorylation of Smad-3 (*Figure* 7C and 7D); thus, suggesting that Smad-2 is the predominant intracellular pathway regulating the activin-A effect on Atrogin-1 and MuRF-1 in the gastrocnemius of the α-KO mice. In support of this, when

DOI: 10.1002/jcsm.12031

Figure 4 Activin-β_C overexpression attenuates Beclin-1 and p62 levels in the α-KO mice. Quantification of western blots signal intensities for Beclin-1 and p62/SQSTM1 in the gastrocnemius of 8 week-old males (a) and females (b) mice *n* = 4 per group. Normalized values are expressed as relative intensities (800 nm channel/700 nm channel) to WT. Signals from Beclin-1 and p62 appear as green fluorophores, and signals from GAPDH appear as red fluorophores. Values are mean ± SEM. ns = $P > 0.05$; * $P \leq 0.05$; ** $P \leq 0.01$; **** $P \leq 0.0001$.

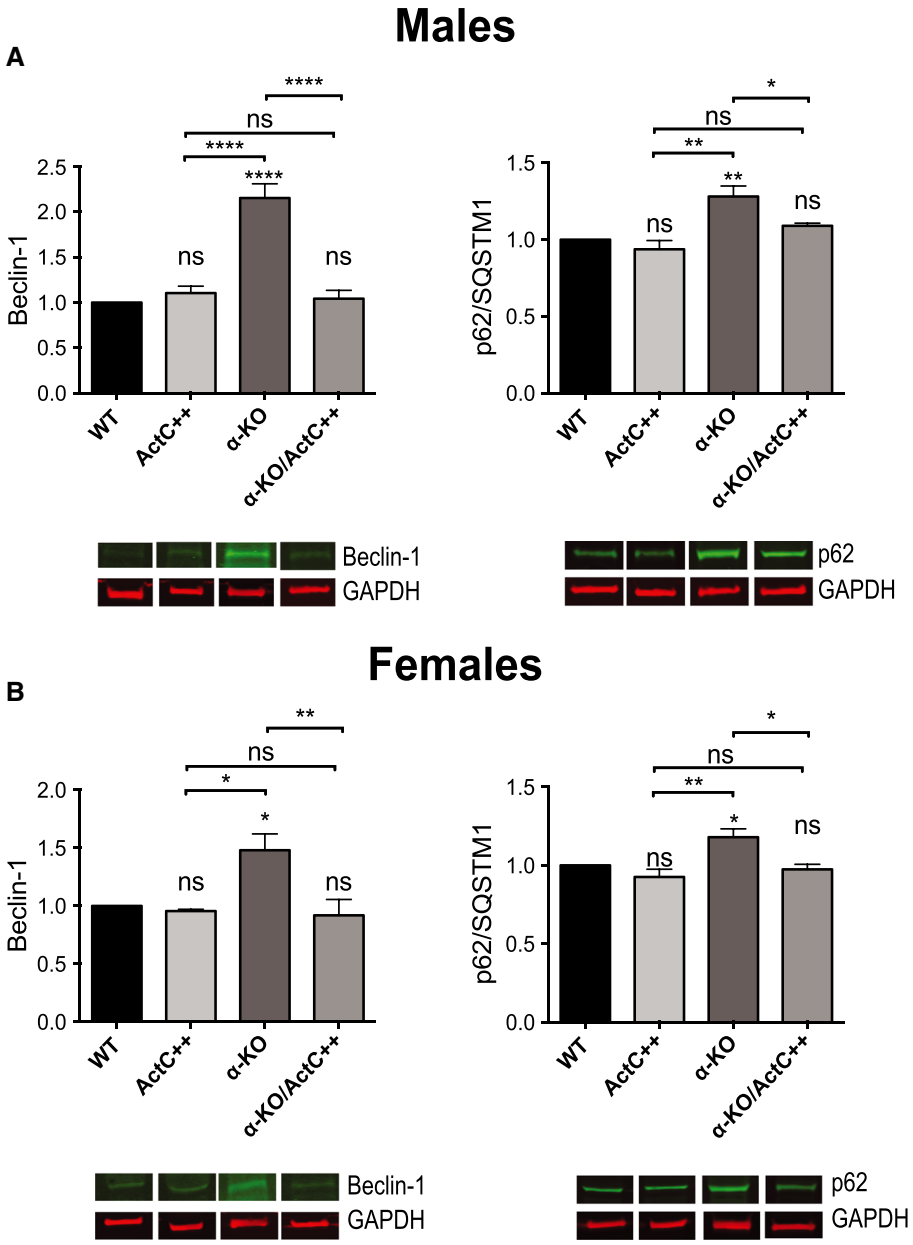

activin-β_C was overexpressed, a clear reduction of Smad-2 phosphorylation was evident in the α-KO mice.

Additionally, histological assessment of the gastrocnemius (*Figures* 8 and 9) showed that the average cross-sectional area in the α-KO mice was reduced compared with the WT controls in male (−63% $P < 0.01$) and female (−60% $P < 0.01$) mice (*Figure* 10A and 10B). Overexpression of activin-β_C abrogated this decline, restoring the muscle cross-sectional area to levels not statistically different compared with WT controls.

Activin-β_C overexpression has no impact on testosterone, estradiol, or bone density in the α-KO mice

A relationship between inflammation and bone disease has been established in a variety of models of inflammatory disease, as well as human studies.[27–29] Therefore, we assessed the impact of elevated inflammatory cytokines in the α-KO mice on bone density. Femora from WT, ActC++, α-KO, and

DOI: 10.1002/jcsm.12031

Figure 5 Activin-β_C overexpression does not affect the LC3A/B-I or LC3A/B-II levels in the α-KO mice. Quantification of western blots signal intensities for LC3A/B-I and LC3A/B-II in the gastrocnemius of 8 week-old males (a) and females (b) mice *n* = 4 per group. Normalized values are expressed as relative intensities (800 nm channel/700 nm channel) to WT. Signals from LC3A/B appear as green fluorophores, and signals from GAPDH appear as red fluorophores. Values are mean ± SEM. ns = $P > 0.05$; ** $P \leq 0.01$; ** $P \leq 0.001$; *** $P \leq 0.001$; **** $P \leq 0.0001$.

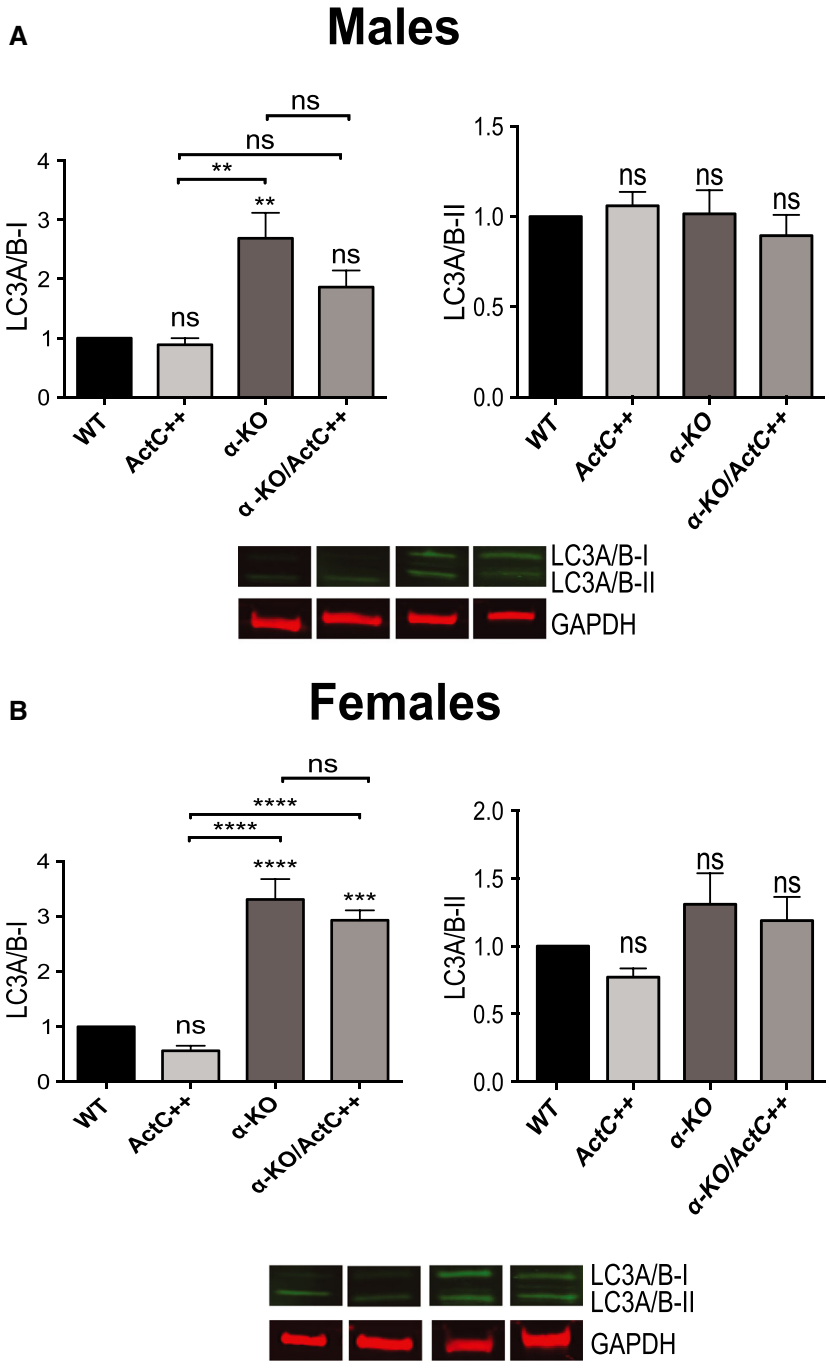

α-KO/ActC++ mice were analyzed. A reduction of bone density was noted in both male (0.33 ± 0.01 g/cm^3 $P < 0.0001$) and female (0.33 ± 0.02 g/cm^3 $P < 0.02$) α-KO mice compared with the WT control animals. No difference was noted between the α-KO and α-KO/ActC++ in both male and female mice (*Figure* 10C and 10D).

Testosterone and estradiol serum levels were also assessed in male (*Figure* 10E) and female (*Figure* 10F)

Figure 6 Activin-β_C overexpression does not affect the myostatin levels in the α-KO mice. Quantification of western blots signal intensities for myostatin in 8 week-old males (c) and females (d) mice *n* = 4 per group. Normalized values are expressed as relative intensities (800 nm channel/700 nm channel) to WT. Signals from Myostatin appear as green fluorophores, and signals from GAPDH appear as red fluorophores. Values are mean ± SEM. ns = $P > 0.05$; * $P \leq 0.05$.

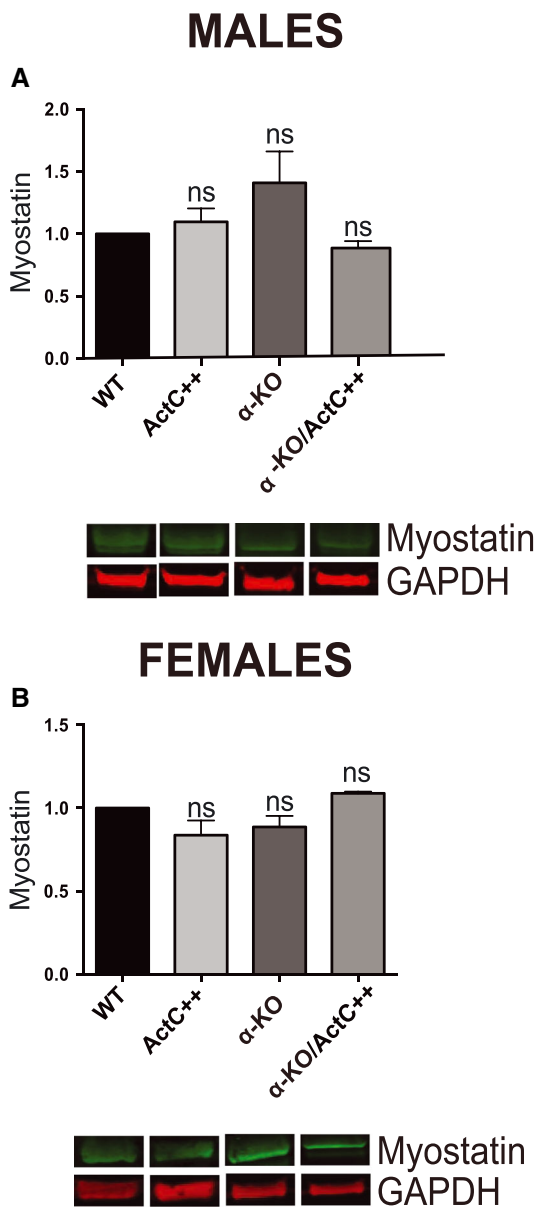

mice to determine their potential contribution in the changes in bone density of the α-KO and α-KO/ActC++ groups compared with the WT controls. Results showed no statistically significant changes in both testosterone and estradiol serum levels between the α-KO and α-KO/ActC++ mice.

Discussion

Although cachexia represents a debilitating syndrome affecting the majority of cancer patients and is negatively correlated with the patient's quality of life, the biological mechanism leading to this multifaceted syndrome is poorly understood. A deeper understanding of the pathophysiology of cachexia and its progression is needed in order to lead to development of new therapies, as cachexia is usually considered a causative factor of cancer patient mortality and morbidity.[1]

Given the urgent need for an effective treatment to combat cachexia, animal models have an essential role not only for assessing the efficacy and safety of a potential treatment but also to better understand biological mechanisms involved in muscle wasting and cancer cachexia.[30] The inhibin-α deficient (α-KO) mouse model used in this study was first described by Matzuk *et al.* and it clearly showed the importance of activins: members of the TGF-β family ligands, in the progression of cancer cachexia.[7] After genetic removal of the inhibin-α subunit, these mice develop gonadal sex-cord stromal tumours within 6 weeks, causing death in males and females in 12 and 17 weeks, respectively. The development of gonadal cancers is followed by a cancer cachexia-like wasting syndrome that is associated with weight loss and stomach and liver related problems.[7] The gonadal tumours secrete high levels of activin-A and inflammatory cytokines, which are responsible for the pronounced effect on weight loss.

Zhou *et al.* reported the importance of the activin signalling pathway mediated by the activin type-2 receptor (ActRIIB) to reverse cachexia and showed that using a decoy receptor not only abrogates the wasting process in skeletal muscle and heart but also increases survival. Therefore, activins and possibly other members of the TGF-β superfamily clearly have a central role in the pathophysiology of cancer cachexia with the activin/myostatin signalling pathway being identified as a suitable candidate to reverse cancer-associated cachexia in murine models.[10]

A study conducted by our group described for the first time a new activin-A antagonist: activin-β_C. This protein acts as an activin-A antagonist both *in vitro* and *in vivo*.[18] Based on this evidence, we used mice overexpressing activin-β_C crossed with α-KO mice to assess the biological effect of activin-β_C overexpression on the onset of gonadal tumors and cancer-associated cachexia. We did find that the α-KO/ActC++ mice had no significant weight loss, increased survival, and that the gonadal tumor formation was modified.[19] Building on our previous study, we wanted to characterize the biological mechanism by which the α-KO/ActC++ showed increased survival, assessing for the first time the effect of overexpression of activin-β_C on muscle degradation, bone density, and inflammatory and hormonal profile.

Figure 7 Activin-β_C overexpression reduces phosphorylated Smad2, but not Smad3 in the α-KO mice. Quantification of western blots signal intensities for Smad-2/p-Smad2 and Smad-3/p-Smad-3 in the gastrocnemius of male (a, c) and female (b, d) mice, 8 week-old mice *n* = 4 per group. Normalized values are expressed as relative intensities (800 nm channel/700 nm channel) to WT. Signals from Smad-2/p-Smad-2, Smad-3 and p-Smad3 appear as green fluorophores, and signals from GAPDH appear as red fluorophores. Values are mean ± SEM. ns = $P > 0.05$; * $P \leq 0.05$; ** $P \leq 0.01$; *** $P \leq 0.001$; **** $P \leq 0.0001$.

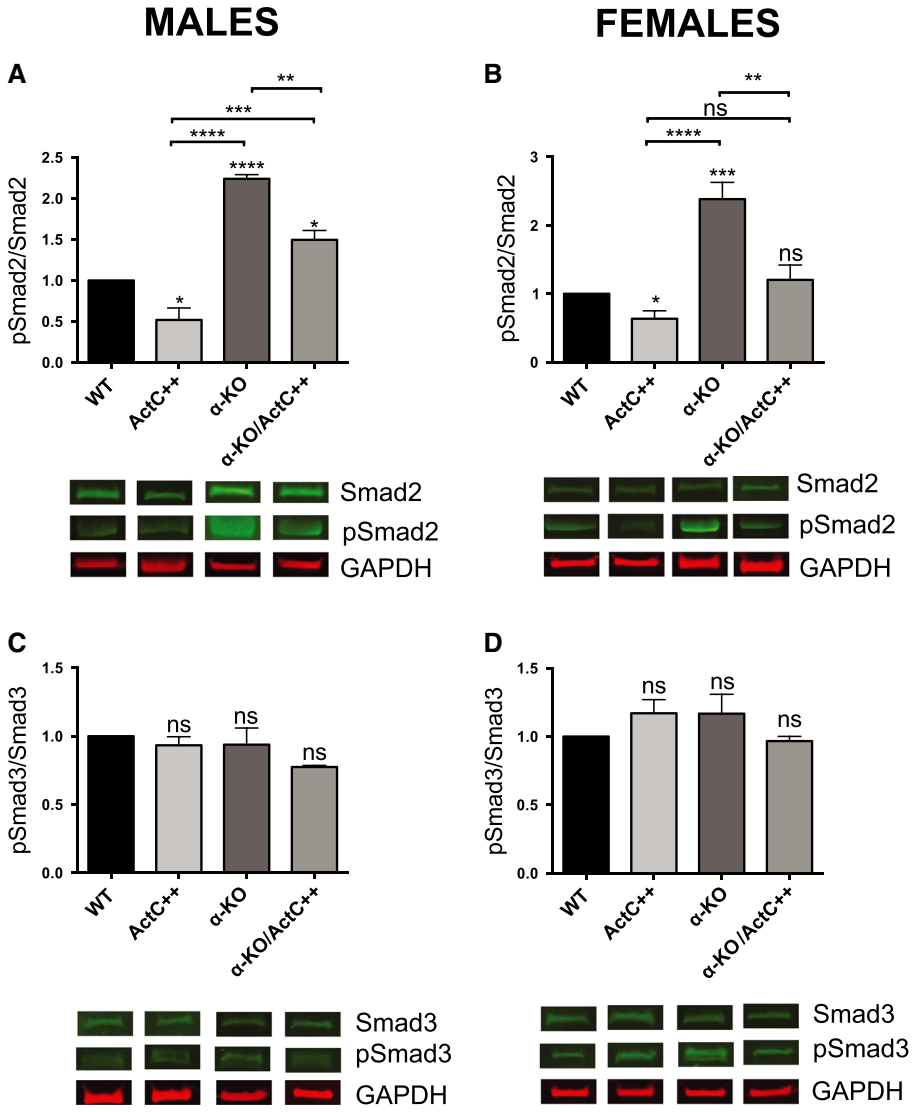

Our findings revealed a previously unappreciated function for activin-β_C on muscle metabolism and activation of transcription factors involved in muscle protein degradation. We defined the molecular mechanism by which activin-β_C increases survival and ameliorates the muscle wasting phenotype in the α-KO mice. We confirmed that overexpression of activin-β_C reduced serum activin-A and it also reduced inflammatory cytokines, factors recognized to have an essential role in the progression of cancer-associated cachexia and directly involved in triggering the mechanism of wasting. Despite a significant reduction in the serum levels of activin-A in both male and female α-KO/ActC++ mice vs. the α-KO counterpart, the current study revealed that this reduction is less marked in the female mice. Interestingly, this trend reflects the tumor growth data (*Figure* 1A and 1B). In fact, gonadal weight in the males α-KO/ActC++ was not statistically significant vs. WT mice, while in the female α-KO/ActC++, a statically significant change was still present vs. the WT counterpart.

It has been hypothesized that the gonadal tumours developed in the α-KO mice are responsible for the secretion of high levels of activin-A and inflammatory cytokines such as tumor necrosis factor (TNF-α), interleukin-6 (IL-6), and interferon-gamma (IFN-γ). Our data support this hypothesis and show that the modulation of gonadal cancers by overexpressing activin-β_C also has a previously unappreciated

Figure 8 Hematoxylin and eosin staining of gastrocnemius fibers in a transverse section from WT (a), ActC++ (b), α-KO (c) and α-KO/ActC++ (d) male mice. Scale bar 100 μM, 20× objective.

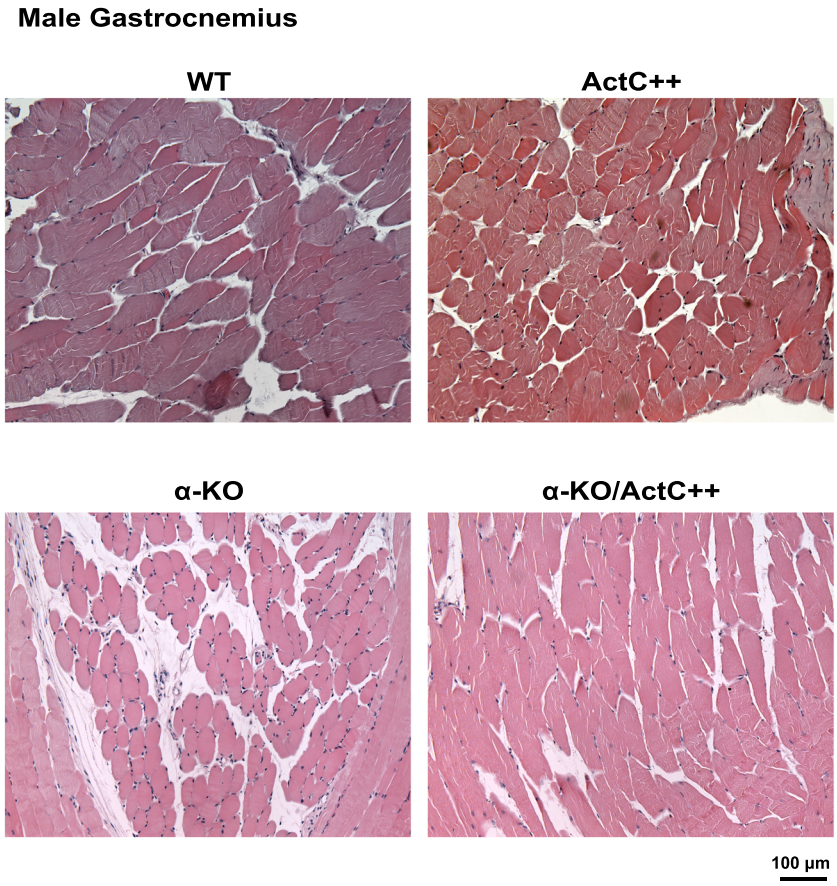

impact on inflammatory cytokines, resulting in a significant biological effect. Based on our previous study in which we showed that activin-β_C is an activin/myostatin signalling pathway antagonist at the receptor level,[31] we conclude that the effect of activin-β_C on cancer-cachexia is likely to act via a two-fold mechanism: modulation of gonadal tumor growth and antagonistic effect on the signaling pathway activated by TGF-β ligands myostatin and activin-A (previously showed to be aberrant in cancer cachexia) in gonadal and extra-gonadal tissues like skeletal muscle.

Reduced levels of Atrogin-1 and MuRF-1 were evident in the α-KO/ActC++ compared with the α-KO mice. Both myostatin and activin bind to the ActRIIB to initiate a signalling cascade leading to an increased expression of Atrogin-1 and MurRF-1, resulting in increased degradation of myofibrillar proteins through the ubiquitin-proteasome pathway. In our previous studies, we showed that activin-β_C could antagonize the activin signaling pathway both *in vivo* and *in vitro*, not only forming a dimer complex activin-AC and therefore reducing the bioactive levels of activin-A but also binding to the ActRIIA and IIB and acting as a receptor antagonist *in vitro*.[18,19,31] These data support the findings described in the current study; in fact, overexpression of activin-β_C attenuated the ubiquitin-proteasome system, decreasing the expression of both Atrogin-1 and MuRF-1.

We also showed that the expression of the autophagic-lysosomal pathway associated effectors Beclin-1, p62, and LC3A/B-I was increased in the α-KO mice, thus suggesting an increased proteolytic activity that contributes to the loss of muscle protein in cancer cachexia.

Overexpression of activin-β_C attenuated this activation, decreasing the expression of Beclin-1 and p-62 in the α-KO/ActC++ mice vs. the α-KO counterpart. However, overexpression of activin-β_C did not reduce the protein levels of LC3A/B-I in the α-KO/ActC++ mice vs. the α-KO counterpart.

These data suggest an activation of the autophagic pathway in the α-KO mouse model of cancer cachexia and support previous evidence suggesting that autophagy significantly contributes to muscle wasting,[17] thus suggesting the autophagic-proteolytic system as a possible target for therapeutic strategies.

Additionally, in the α-KO/ActC++ mice, the Smad2 phosphorylation and therefore activation was reduced compared with the α-KO animals. This has important biological consequences for protein degradation in muscles, as Smad-2

Figure 9 Hematoxylin and eosin staining of gastrocnemius fibers in a transverse section from WT (a), ActC++ (b), α-KO (c) and α-KO/ActC++ (d) female mice. Scale bar 100 μM, 20× objective.

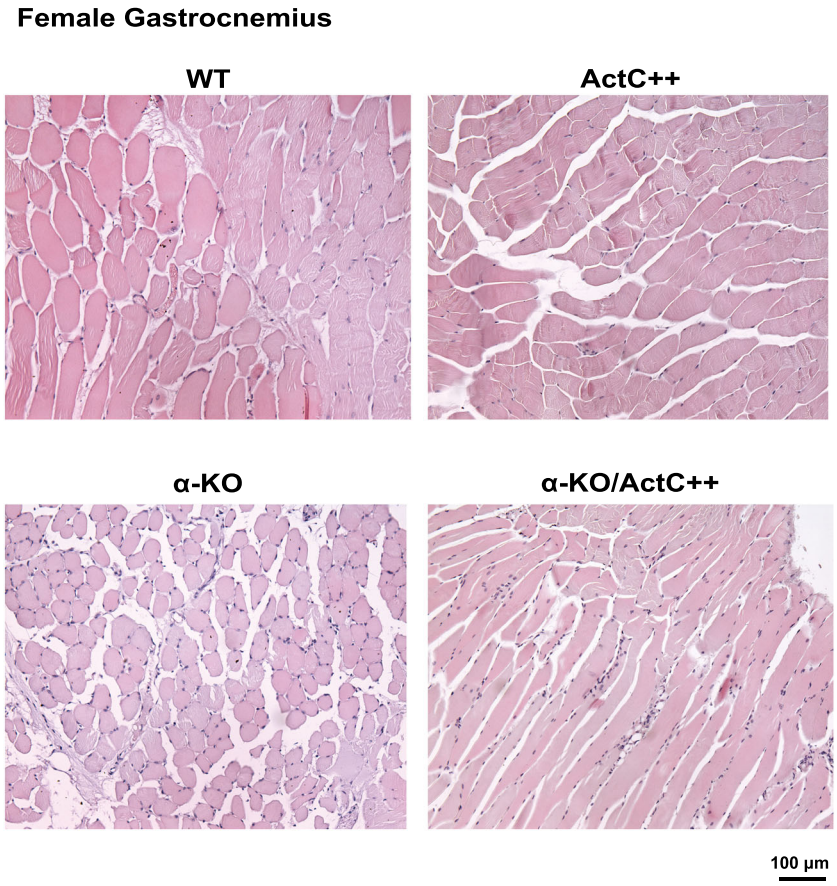

phosphorylation stimulates activation of FOXO3a, which is then de-phosphorylated and moves to the nucleus, where it activates the expression of both Atrogin-1 and MuRF-1.[11] A beneficial effect of activin-β_C was also noted in the gastrocnemius tissue, with α-KO/ActC++ mice showing less morphometric signs of muscle atrophy.

Inflammation of almost any cause is usually associated with bone loss.[32] It has been shown that some inflammatory cytokines have a negative effect on bone formation, inducing osteoclast formation. TNF-α, for example, plays a critical role in enhancing osteoclast-mediated bone resorption by interacting with the receptor activator of nuclear factor-kB ligand.[33] IL-6 is another important inflammatory cytokine, which has a negative impact on the bone metabolism supporting osteoclasts via the interaction with mesenchymal cells.[34,35] Hormonal alterations themselves play an important role for both skeletal development and maintenance. Androgens and estrogens, for example, have been shown to have central roles for bone homeostasis in men and rodents.[36] Previous studies have shown that the effects of androgens on the bone metabolism may be mediated by the androgen receptor or via the aromatization of androgen to estrogens.[37]

Additionally, inhibin-α has an impact on the bone metabolism. It has previously been hypothesized that continuous exposure to inhibin is anabolic to the skeleton. However, lack of inhibin leads to an acceleration of osteoblast and osteoclast development, leading to an increase in bone turnover.[38] Therefore, with the present study, we investigated if changes in the inflammatory cytokines and hormonal alterations had any effect on bone density and whether overexpression of activin-β_C was associated with this effect. No difference was noted between the WT and ActC++ groups; however, both the α-KO and α-KO/ActC++ mice had reduced bone density compared with the WT age-matched controls. Serum levels of testosterone and estradiol did not differ in the α-KO and α-KO/ActC++ groups; therefore, the reduced bone density observed in these mice is likely to be a consequence of the high levels of inflammatory cytokines and lack of inhibin-α. We speculate that the reduced bone density noted in α-KO/ActC++ compared with the α-KO mice, despite a reduction in inflammatory cytokines reported in the α-KO/ActC++ mice, is caused by the lack of inhibin-α, as the hormonal profile did not show significant changes. These findings, taken together, suggest that activin-β_C does not play an independent central role in the regulation of bone metabolism.

Figure 10 Activin-βC overexpression reverses fiber atrophy and does not affect the bone density or the hormonal profile in the α-KO mice. Morphometric analysis of the gastrocnemius showing the gastrocnemius average fiber area (μm2) from male (a) and female (b) 8 week-old mice, *n* = 4 per group. Bone density (g/cm3) in male (c) and female (d) mice. Eight week-old mice, *n* = 4–8 per group. Serum testosterone and estradiol levels in male (e) and female (f) mice. 8 week-old mice, *n* =3 per group. Values are mean ± SEM. ns = $P > 0.05$; * $P \leq 0.05$; ** $P \leq 0.01$; *** $P \leq 0.001$; **** $P \leq 0.0001$.

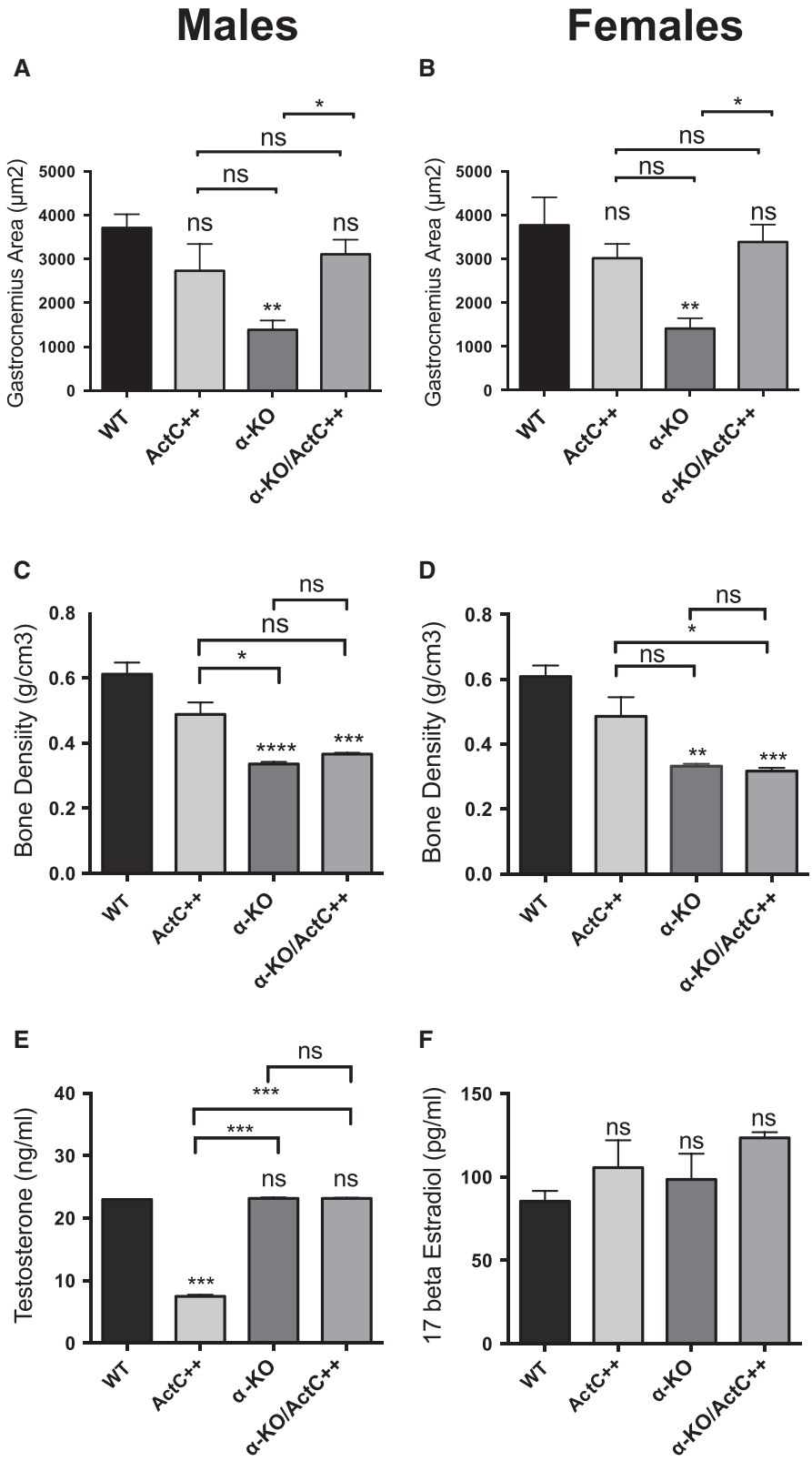

DOI: 10.1002/jcsm.12031

Conclusion

This study shows the importance of activin signaling in cancer-associated cachexia, providing further rationale for the therapeutic potential of anti-activin therapies. The data support the importance of activin-β_C as a regulator of activin-A bioactivity *in vivo*. We showed for the first time that activin-β_C has an effect in modulating the catabolic factors, Atrogin-1 and MuRF-1, which are responsible for triggering the mechanism of wasting not only in cancer-associated cachexia but also in many other catabolic conditions. Additionally, we showed that activin-β_C has an effect in modulating two of the most important markers associated with the autophagic-lysosomal pathway, which has been suggested to contribute to muscle wasting in different experimental conditions, such as denervation, starvation, and sepsis.

Overexpression of activin-β_C in the α-KO mouse model of cancer-associated cachexia showed a biological effect, reducing circulating levels of activin-A, inflammatory cytokines involved in the mechanism of wasting and ameliorating the muscle loss. Further studies are necessary in order to clarify if the effect of activin-β_C is likely to be anabolic only when deregulation of activin signalling is present, or if its use might be beneficial in conditions such as muscoskeletal disorders not directly related to the activin signalling pathway.

Acknowledgements

The authors thank Sylvia Zellhuber-McMillan and Geeta Singh (University of Otago) for their technical assistance and the staff of the Histology Laboratory (Deparment of Pathology – University of Otago) for processing and sectioning the histological slides.

F.E.M. designed the study, carried out data collection, data analysis and wrote the manuscript. E.G. designed the study and wrote the manuscript. G.R. designed the study and revised the manuscript. All authors have read and approved the final version.

The authors of this manuscript certify that they comply with the ethical guidelines for authorship and publishing in the Journal of Cachexia, Sarcopenia, and Muscle 2010;1:7–8 (von Haehling S, Morley JE, Coats AJ and Anker SD).

Funding

This work was supported by a National Health and Medical Research Council Australia Project Grant (1008058; to G.R.) and a University of Otago Doctoral Scholarship (to F.E.M.).

Conflict of interest

The authors declare there is no conflict of interest relating to this work.

Supporting information

Supporting information may be found in the online version of this article.

Figure S1. Overexpression of activin-βC modulates ovarian but not testicular weight when an advanced stage of tumor development is present. Male (a) and female (b) gonadal weight in 12–17 week-old mice. Values shown represent mean ± SEM. ns = $p > 0.05$; ** $p > 0.01$; ****$p > 0.0001$.

References

1. Fearon K, Strasser F, Anker SD, Bosaeus I, Bruera E, Fainsinger RL, et al. Definition and classification of cancer cachexia: an international consensus. *Lancet Oncol* 2011;**12**:489–495.
2. Yavuzsen T, Davis MP, Walsh D, LeGrand S, Lagman R. Systematic review of the treatment of cancer-associated anorexia and weight loss. *J Clin Oncol* 2005;**23**: 8500–8511.
3. Argilés JM, Moore-Carrasco R, Fuster G, Busquets Sl, López-Soriano FJ. Cancer cachexia: the molecular mechanisms. *Int J Biochem Cell Biol* 2003;**35**:405–409.
4. Lee S-J, McPherron AC. Regulation of myostatin activity and muscle growth. *Proc Natl Acad Sci* 2001;**98**:9306–9311.
5. Schuelke M, Wagner K, Stolz L, Hubner C, Riebel T, Komen W, et al. Myostatin mutation associated with gross muscle hypertrophy in a child. *New England Journal of Medicine* 2004;**350**:2682–2688.
6. Zimmers T, Davies M, Koniaris L, Haynes P, Esquela A, Tomkinson K, et al. Induction of cachexia in mice by systemically administered myostatin. *Science* 2002;**296**:1486–1488.
7. Matzuk M, Finegold M, Mather J, Krummen L, Lu H, Bradley A. Development of cancer cachexia-like syndrome and adrenal tumors in inhibin-deficient mice. *Proc Natl Acad Sci* 1994;**91**:8817–8821.
8. Lee S.-J, Lee Y.-S, Zimmers TA, Soleimani A, Matzuk MM, Tsuchida K, et al. Regulation of muscle mass by follistatin and activins. *Molecular endocrinology* 2010;**24**:1998–2008.
9. Benny Klimek ME, Aydogdu T, Link MJ, Pons M, Koniaris LG, Zimmers TA. Acute inhibition of myostatin-family proteins preserves skeletal muscle in mouse models of cancer cachexia. *Biochemical and Biophysical Research Communications* 2010;**391**:1548–1554.
10. Zhou X, Wang JL, Lu J, Song Y, Kwak KS, Jiao Q, et al. Reversal of cancer cachexia and muscle wasting by ActRIIB antagonism leads to prolonged survival. *Cell* 2010;**142**:531–543.
11. Tisdale MJ. Reversing cachexia. *Cell* 2010;**142**:511–512.
12. Goodman CA, McNally RM, Hoffmann FM, Hornberger TA. Smad3 induces atrogin-1, inhibits mTOR and protein synthesis, and promotes muscle atrophy in vivo. *Mol Endocrinol* 2013;**27**:1946–1957.
13. Cohen S, Brault JJ, Gygi SP, Glass DJ, Valenzuela DM, Gartner C, et al. During muscle atrophy, thick, but not thin, filament components are degraded by MuRF1-dependent ubiquitylation. *J Cell Biol* 2009;**185**:1083–1095.

14. Sandri M. Autophagy in skeletal muscle. *FEBS Lett* 2010;**584**:1411–1416.
15. den Kamp CMO, Langen RC, Snepvangers FJ, de Theije CC, Schellekens JM, Laugs F, et al. Nuclear transcription factor κ B activation and protein turnover adaptations in skeletal muscle of patients with progressive stages of lung cancer cachexia. *Am J Clin Nutr* 2013;**98**:738–748.
16. Tardif N, Klaude M, Lundell L, Thorell A, Rooyackers O. Autophagic-lysosomal pathway is the main proteolytic system modified in the skeletal muscle of esophageal cancer patients. *Am J Clin Nutr* 2013; **98**:1485–1492.
17. Penna F, Costamagna D, Pin F, Camperi A, Fanzani A, Chiarpotto EM, et al. Autophagic degradation contributes to muscle wasting in cancer cachexia. *Am J Pathol* 2013; **182**:1367–1378.
18. Gold E, Jetly N, O'Bryan MK, Meachem S, Srinivasan D, Behuria S, et al. Activin C antagonizes activin a in vitro and overexpression leads to pathologies in vivo. *Am J Pathol* 2009;**174**:184–195.
19. Gold E, Marino FE, Harrison C, Makanji Y, Risbridger G. Activin-βc reduces reproductive tumour progression and abolishes cancer-associated cachexia in inhibin-deficient mice. *J Pathol* 2013;**229**:599–607.
20. Matzuk MM, Finegold MJ, Su J-GJ, Hsueh AJW, Bradley A. [alpha]-Inhibin is a tumour-suppressor gene with gonadal specificity in mice. *Nature* 1992;**360**:313–319.
21. Musarò A, McCullagh K, Paul A, Houghton L, Dobrowolny G, Molinaro M, et al. Localized Igf-1 transgene expression sustains hypertrophy and regeneration in senescent skeletal muscle. *Nat Genet* 2001;**27**:195–200.
22. Gangopadhyay SS. Systemic administration of Follistatin288 increases muscle mass and reduces fat accumulation in mice. *Sci Rep* 2013;**3**:2441.
23. Solomon V, Baracos V, Sarraf P, Goldberg AL. Rates of ubiquitin conjugation increase when muscles atrophy, largely through activation of the N-end rule pathway. *Proc Natl Acad Sci* 1998;**95**:12602–12607.
24. Kwak KS, Zhou X, Solomon V, Baracos VE, Davis J, Bannon AW, et al. Regulation of protein catabolism by muscle-specific and cytokine-inducible ubiquitin ligase E3α-II during cancer cachexia. *Cancer Res* 2004; **64**:8193–8198.
25. Funderburk SF, Wang QJ, Yue Z. The Beclin 1–VPS34 complex–at the crossroads of autophagy and beyond. *Trends Cell Biol* 2010;**20**:355–362.
26. Klionsky DJ, Abdalla FC, Abeliovich H, Abraham RT, Acevedo-Arozena A, Adeli K, et al. Guidelines for the use and interpretation of assays for monitoring autophagy. *Autophagy* 2012;**8**:445–544.
27. Gough A, Emery P, Holder R, Lilley J, Eyre S. Generalised bone loss in patients with early rheumatoid arthritis. *Lancet* 1994; **344**:23–27.
28. Bernstein CN, Blanchard JF, Leslie W, Wajda A, Yu BN. The incidence of fracture among patients with inflammatory bowel disease: a population-based cohort study. *Ann Intern Med* 2000;**133**:795–799.
29. Bultink IE, Lems WF, Kostense PJ, Dijkmans BA, Voskuyl AE. Prevalence of and risk factors for low bone mineral density and vertebral fractures in patients with systemic lupus erythematosus. *Arthritis & Rheumatism* 2005;**52**:2044–2050.
30. DeBoer MD. Animal models of anorexia and cachexia. *Expert Opin Drug Discovery* 2009;**4**:1145–1155.
31. Marino FE, Risbridger G, Gold E. The inhibin/activin signalling pathway in human gonadal and adrenal cancers. *Mol Hum Reprod* 2014;**20**:1223–1237.
32. Hardy R, Cooper M. Bone loss in inflammatory disorders. *J Endocrinol* 2009;**201**: 309–320.
33. Schett G. Effects of inflammatory and anti-inflammatory cytokines on the bone. *Eur J Clin Invest* 2011;**41**:1361–1366.
34. Udagawa N, Takahashi N, Katagiri T, Tamura T, Wada S, Findlay DM, et al. Interleukin (IL)-6 induction of osteoclast differentiation depends on IL-6 receptors expressed on osteoblastic cells but not on osteoclast progenitors. *J Exp Med* 1995; **182**:1461–1468.
35. Ishimi Y, Miyaura C, Jin CH, Akatsu T, Abe E, Nakamura Y, et al. IL-6 is produced by osteoblasts and induces bone resorption. *J Immunol* 1990;**145**:3297–3303.
36. Goulding A, Gold E. Effects of chronic prednisolone treatment on bone resorption and bone composition in intact and ovariectomized rats and in ovariectomized rats receiving β-estradiol. *Endocrinology* 1988; **122**:482–487.
37. Vandenput L, Ederveen AG, Erben RG, Stahr K, Swinnen JV, Van Herck E, et al. Testosterone prevents orchidectomy-induced bone loss in estrogen receptor-α knockout mice. *Biochem Biophys Res Commun* 2001;**285**:70–76.
38. Gaddy D. Inhibin and the regulation of bone mass. *Curr Osteoporos Rep* 2008;**6**:51–56.